Measurement of suspension velocity in slurries and pastes using impedance imaging

by R.A. Williams* and G. Vilar*

Synopsis

Electrical impedance tomographic methods have been applied to a variety of mineral and chemical processes in the laboratory and on plant. This review paper surveys technical developments in measurement methods to enable quantitative extraction of key process information in the form of mapping of concentration profiles, mixture homogeneity and suspension velocity. The methods for determining velocity are summarized, since this is of especial interest when applied to opaque systems where most conventional optically based measurements fail. A recent significant development is the use of ultra-high speed measurement that now allows velocity vectors to be extracted for fast moving mixtures and fluids (up to several metres per second). New data are reported pertinent to low and high solids concentration flow in pipelines. Use of the methods offer improvements to design of such systems but also points to the use of tomographic electrical sensor as online flow measurement and fault detection. This offers new opportunities for applications and benefits in the design and monitoring of mineral slurries and sludges.

Introduction

Measurement of the properties of fast or slow moving opaque slurries is difficult since many conventional sensors are often based on optical methods. Electrical tomographic sensing can provide an alternative approach[1]. By deploying multiple sensors and detectors and utilizing different forms of analysis of the resultant signals, new information can be extracted. This review seeks to highlight the type of information that can be obtained for mineral slurries and pastes. Details of the principles of the measurement methods and analysis can be found elsewhere[2]. Outcomes of the use of tomographic sensors results in benefits in a range of areas including:

- Improved quality control and product design arising from micro-scale characterization of properties of products;
- Evolution of new process models resulting in improved process design, arising from accurate verification of models (e.g. discrete element, fluid dynamics, empirical reactions/scale up);
- Facilitation of more quantitative flow measurement through measurement of phase concentration and velocity that has not been possible previously;
- Diagnosis of operation problems in pilot and industrial plants;
- Early detection of faults enabled through having *in-situ* sensors and from knowledge gained through spatial-temporal tomographic approach, especially relevant to reaction kinetics, onset of blockages;
- Process control, based on key parameters that cannot be assessed using conventional single point measurements.

The review focuses on benefits arising in a range of operations that utilize tomographically-derived data on particle concentration and velocity that can be related to practical process and flow models[3]. Application examples presented below describe the hydraulic transportation of slurries in pipelines and separators and the behaviour of concentrated pastes. Mixing in stirred tank reactors and pulsed (oscillatory) pipe reactors, both involving complex flows. The future prospects for use of ultra-high speed tomographic data collection are explored for these systems.

Hydraulic transportation and swirling flows

In mineral processing, there are many applications requiring monitoring of solids, flow rate in solids–liquid flows. Two examples that have received attention in the minerals sector have been monitoring of clay-based drilling muds for the oil industry and monitoring of long-distance hydraulic conveying systems[2,4,5].

---

* *Institute of Particle Science and Engineering, School of Process, Environmental and Materials Engineering, University of Leeds, UK.*

© *The Southern African Institute of Mining and Metallurgy, 2008. SA ISSN 0038–223X/3.00 + 0.00. This paper was first published at the SAIMM Symposium,* Tomography, *25 July 2008.*

In drilling cuttings, as in multiphase oil processing, there is a great need for methods that can measure the velocity and concentration of a given phase. The product of multiplying the ‘velocity’ by the ‘concentration’ may not provide a sufficiently accurate estimate of the ‘volumetric flux’ of the phase, since the flow patterns in the pipeline are often complex with swirling and back flows. To this end use of various tomographic tools have been used to obtain better estimates of the phase flux. Electrical impedance tomography (EIT) is particularly suited to monitoring drilling cuttings in water-based muds due to the high conductivity contrast between the drilling mud and the cuttings. An example of such a measurement of the distribution of the local axial velocity of the cuttings was carried out in[6]. Here a dual-plane electrode system enabled accurate measurement of the local solids volume fraction distribution and the axial velocity distribution in solid–liquid flows.

The efficient transportation of particle-bearing fluids through pipes is crucial to many key industries. High slurry velocities have traditionally been used to counteract the tendency of particles to accumulate on the inner pipe wall. The pumping power required to maintain these velocities may cause pipe wall damage, particularly at bends. The introduction of swirl can improve the suspension of pumped slurry and is likely to reduce pipe wear[7]. The major concerns in the application of the swirl-inducing pipe for solids slurry transportation are still the determination of the lowest velocity at which the particles will remain in suspension and the consequence of swirling slurry flow on pipe wear[8]. The swirling decay length downstream of the swirl-inducing pipe is an important parameter in relation to the effective suspension of particles[9]. Descriptions of swirling angle in relation to friction factor of pipe and the dimension of the pipe diameter and decay length have been reviewed[10].

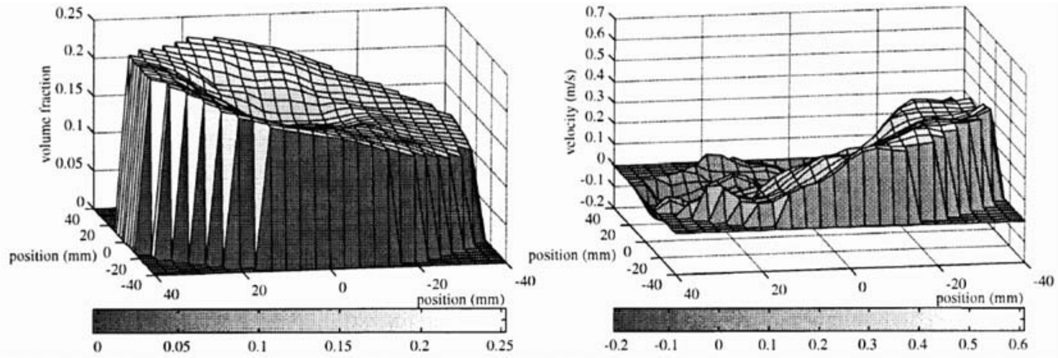

Figure 1—Local solids volume fraction distribution and axial velocity using a dual plane EIT system[6]

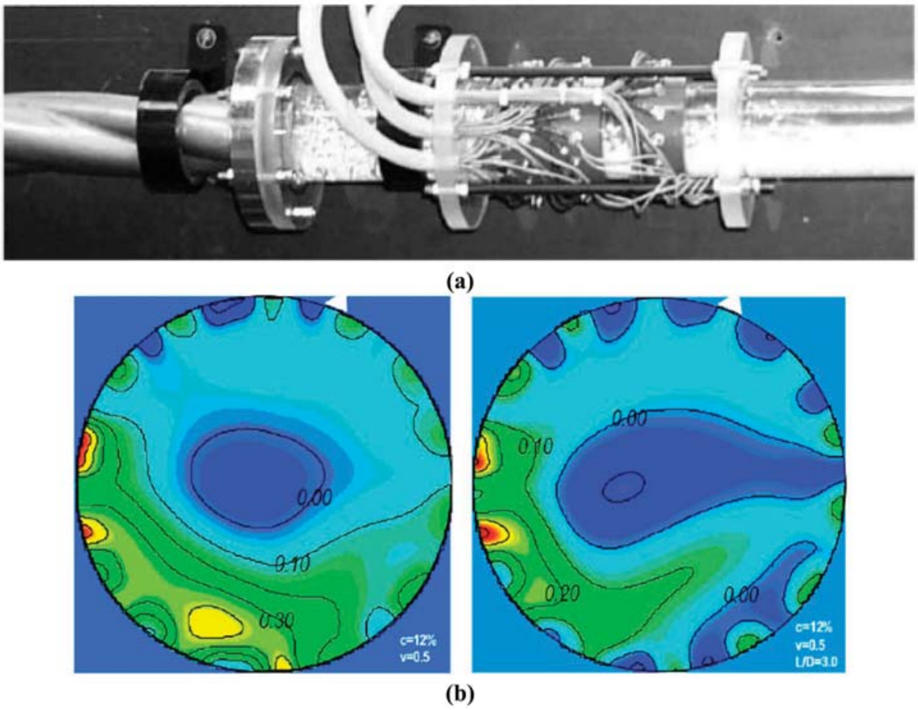

Figure 2—(a) EIT measurement with a dual plane electrode system; (b) axial solids volume fraction distributions from non-swirling flows with estimated concentrations of 2.1 volume %. (left) and at 8.6 volume %. The water flow velocity was 0.5 m/s in both cases[8]

Through the application of EIT the asymmetric solids concentration distribution in horizontal swirling flows can be quantified (Figure2). Particle concentration regimes are reported as a function of the water axial flow velocity and the downstream distance from the swirl-inducing pipe section (L/D)[8].

Without the swirl-inducing pipe, particles at a low velocity (e.g. 0.5 ms^{-1}) tend to clump together. They move in a form of solids slug (i.e. exhibiting saltation) with a considerably lower velocity than the water flow.

At a fixed concentration of 8.6%, effects on the solids distribution or suspension in the downstream pipeline due to velocity change were investigated. Relevant volume fraction distributions at velocities of 1.0, 1.5, 2.0 and 2.5 ms^{-1} at the downstream distances L/D=3.0, 7.4, 17.7 and 23.0 were reconstructed (Figure 3). The use of L/D indicates the relative distance downstream of the swirl section of the pipe expressed in dimensionless form (length divided by pipe diameter). The gravity-driven settling processing of solids distribution due to the decreasing of flow velocity can be observed clearly from these images, particularly at the downstream distance of L/D=17.7. The high concentration in a crescent shape area also moves from the location near the left side of the pipe-wall at L/D=3.0 towards the centre in a ring shape at L/D=17.7 if the flow velocity is sufficiently high (at 2.5 ms^{-1}). With a fixed water velocity of 1 ms^{-1}, solids are well dispersed before the downstream distance L/D=7.4 and the particle is in a fast settling process after the position. The solids have been fully suspended downstream before L/D=23 at the flow velocity of 2.5 ms^{-1}. With fixed downstream distances, effects of velocity may be observed more directly. The changes of solids volume fractions are fairly smooth at all velocities above 1.5 ms^{-1} but fall suddenly at the velocity 1.0 ms^{-1}. At the downstream distance L/D=23, particles were well suspended for a flow velocity above 1.5 ms^{-1}. However, a sudden reduction in the magnitude of the solids volume fraction has occurred when flow velocity has been reduced to 1.0 ms^{-1}. This may indicate that a critical velocity exists in the process, at and above which the vertical component of tangential force suspends particles at greater suspension angles than $\pi/2$. An analysis of suspension angles for a range of flow velocities, supports the existence of a critical velocity in the range 1.0–1.5 ms^{-1} [11]. This work illustrates a good example of quantification of complex flows uniquely facilitated through electrical tomography.

Centrifugal separation

Centrifugal separation is in common use for classification and dewatering in the minerals and other chemical industries. Examples of the use of EIT on hydrocyclones have been reported for mineral[12,13], water and oil/water separation[14,15]

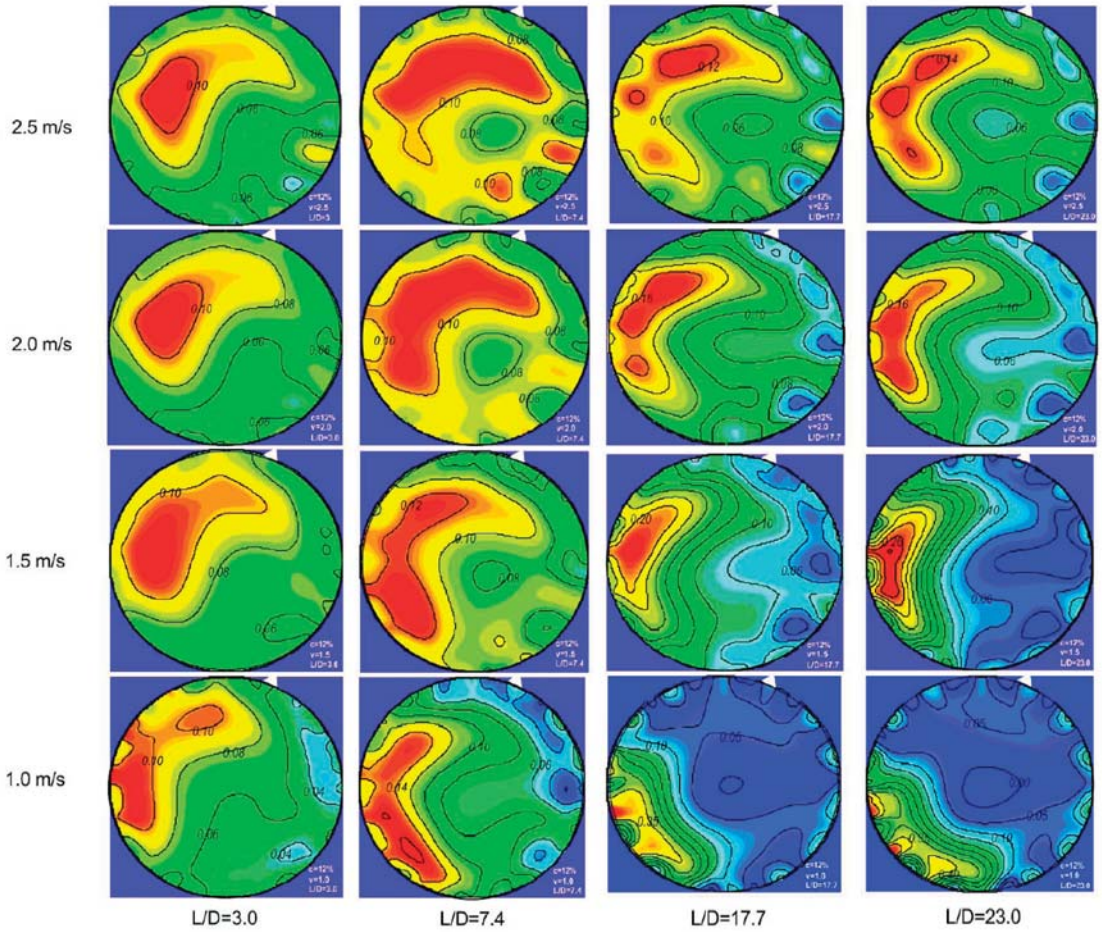

Figure 3—At a fixed concentration of 8.6%, solids volume fraction distribution at downstream positions of L/D= 3.0, 7.4, 17.7 and 23 for water flow velocities of 1, 1.5, 2.0 and 2.5 ms^{-1}. (From [8])

and air/water[16]. Here three distinct applications will be illustrated pertaining to fault detection, online control and process modelling, respectively.

Fault detection

The first application of electrical resistance tomography for online auditing of an industrial hydrocyclone separation is given by[15]. The work demonstrated the retrofitting of electrodes into a commercially available separator and their use in laboratory, pilot-plant and plant-scale investigations of clay refining (Figure 4). A number of new and significant applications are described including: the development of methodologies to allow observation of the occurrence of faults in underflow discharge (spraying, roping, blockage); accurate measurement of the air core size for different operational conditions; and direct calculation of solid concentration profiles based on parametric reconstruction of conductivity data in three dimensions.

The measurement and analysis of the EIT data from the sensor (Figure 4) enable detection of different discharge faults in the hydrocyclone. Figure 5 shows reconstructed images for the top and bottom set of electrode rings installed in the 50 mm unit. The top plane is located just below the vortex finder and the bottom plane is just above the spigot cap.

The different colours shown relate to different relative conductivities from which three fault conditions can be identified. The left-hand pair shows the detection of blockage of the spigot (air is seen as blue colour). The pair in the middle shows the situation when the underflow is roping (high viscous solids concentration, poor cut size). The right-hand pair shows the effect of the spigot experiencing gross wear or detachment of the spigot completely a large air core (blue colour) is seen to develop. No a priori knowledge has been assumed in reconstructing the images shown here, other than the assumption inherent in the linear back projection reconstruction scheme. Using these basic methods, the common fault states in a given hydrocyclone can be diagnosed.

Process control

If the user's knowledge of the process phenomena is used to develop a reconstruction algorithm that is based on a process based model, significant enhancements can be achieved. For example, if the reconstruction seeks to fit the location and diameter of the air core itself then these parameters can be predicted with accuracy and at known confidence levels[14]. To provide an example of this, Figure 6 shows the operation of the system in an industrial setting (Figure 6a) and sample results. An image (inset top right) shows the information that needs to be interpreted if a linear projection is applied to a pixel-based reconstruction. If a parametric approach is used[17] quantitative sizing of the air core can be achieved, as demonstrated in Figure 6b for two different spigots, again as

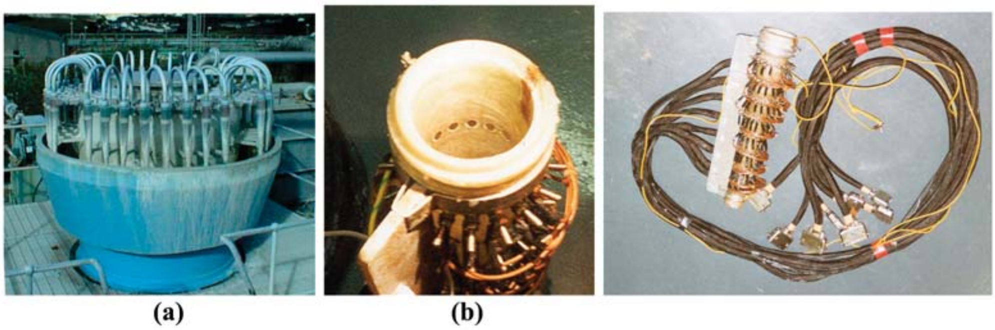

Figure 4—(a) 50 mm diameter hydrocyclones used at IMERYS clay refineries and (b) views of multiple EIT sensor planes installed in a small diameter hydrocyclone. (Taken from [15])

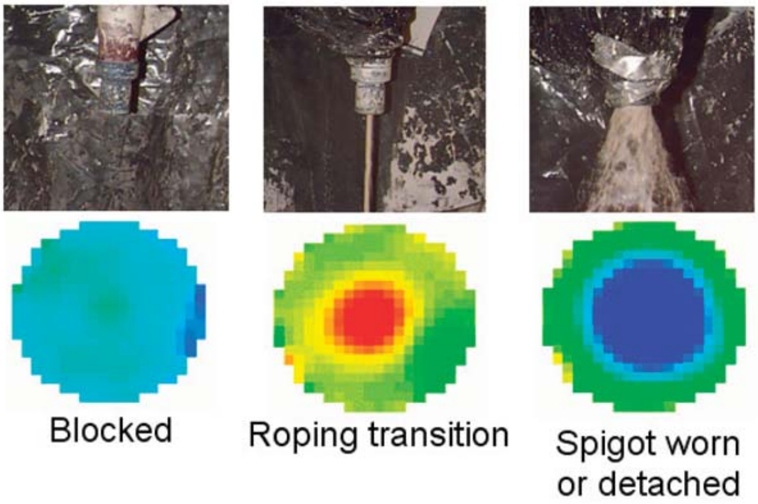

Figure 5—Detail of a spigot in a hydrocyclone and reconstructed impedance measurements for different conditions. (From [15])

a function of pressure drop. The accuracy is very good and sufficient to allow the method to be considered as a mean of wear detection for the spigot itself (since air core size can be related to spigot size).

The approach to image reconstruction, illustrated in Figure 7, can be extended to include fitting the measurements to other system properties, for instance, to deduce the conductivity profiles from which the solid concentration can be inferred. The problem can be expressed in terms of 'fitting parameters' that describe the essential features of the property being sought[14]. For the hydrocyclone this involves estimating the size and location of the air core, and the form of the curve defining the radial solids concentration profile normal to specified positions along the axis of the cyclone. If the air core size is centrally located, then the problem may reduce to solution of 3 or 4 parameters. High conductivity is associated with lower solids concentration.

Process modelling

In more recent work detailed reconstructions of solids concentration within the hydrocyclone[3,12]. This has led to a new understanding of the flow structures within cyclones and especially the role of asymmetry in the flow characteristics[13].

Further use of impedance data to map average solids concentrations has been resolved and compared with size distribution data from which selectivity functions have been computed. Some unpublished results are shown in Figure 8; this enables interpretation of bypassing to be understood.

Handling pastes

Pastes are often encountered during processing of mineral products and in minerals processing as part of cycle associated with dewatering (e.g. filtration) or in preparation of backfill for deep mine disposal or despatch to tailings dams.

The formulation of pastes is a critical area in the above applications since the flow properties of these materials often needs to be characterized or controlled. For example, on backfill paste assurance of the paste homogeneity is critical

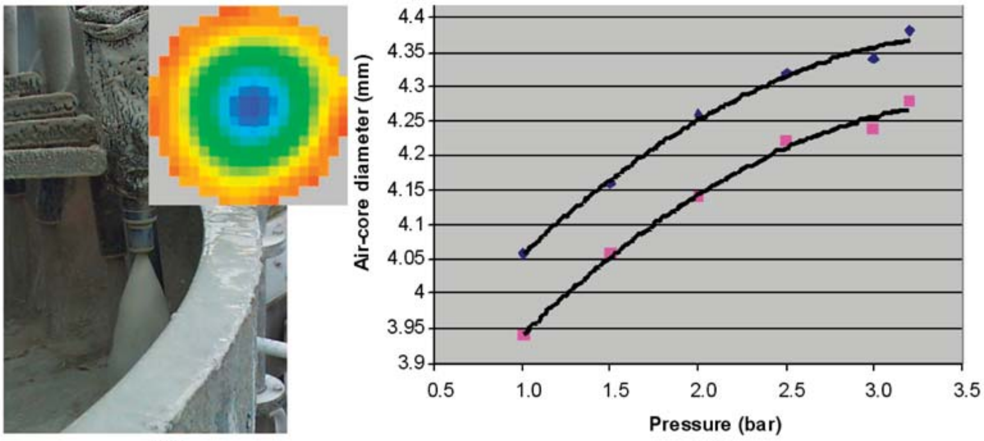

(a) (b)

Figure 6—(a) Industrial EIT measurements with the inset showing a typical resistivity image and (b) derived information of the air core size itseld air core size measurement . Here a parametric reconstruction was used for two different spigot types as a function of pressure drop. (From [15])

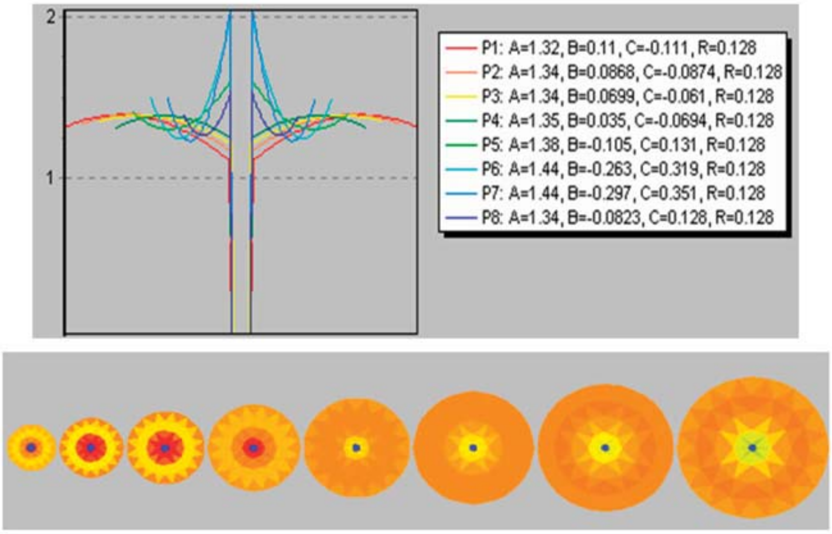

Figure 7—Fitted radial conductivity profiles (top) derived from impedance tomography measurements at 8 positions along a small diameter hydrocyclone using a parametric reconstruction. The corresponding parametric reconstruction images are also shown (bottom) (From [15])

as this determines paste rheology. In addition, work using electrical and X-ray tomography has been applied to aerated pastes and multiphase mixtures prepared in mixers for extrusion.

Extruded materials are of widespread interest for batch and continuous manufacturing in several sectors (agrochemicals, ceramics, solid fuels, polymers and various composite materials including both pastes and emulsions). Electrical tomography has been applied to provide a deeper insight into considering how to formulate products 'in-pipe' and to audit if the structure being formed meets the product specification. This requires in-situ analysis delivering the results within the timescale of the manufacturing process. Often once the product has left the extruder it is too late to effect any change, hence methods for determining and quantifying microstructure are required. The degree of control (actuation) afforded to the operator of the extruder may be limited, and is specific to the process, in which case the in-line methodology can be used to define an optimized operational procedure.

Below is an example in extrusion of an alumina mineral paste, using electrical impedance tomography. This comprises mostly α-alumina with a large range, or spread, of particle sizes that permits high solids loading together with a little clay and a starch binder with water as the liquid phase. There is a strong contrast in electrical resistivity between dry regions of the paste and moist regions since the resistivity is controlled by the moisture content. It is also understood that the liquid phase dominates the extrudability of the paste: paste dilates in key regions to allow greater moisture content and thereby slip planes to be generated. This indicates regions of high moisture at the wall of the barrel permitting slip and so making extrusion more efficient[18].

The speed of the small ram extruder is controlled and operated within the range of 10^{-5}–10^{-3} ms^{-1}. The length of the experiment was fixed to be the time required for the ram to move down to a position where the ram tip was 15 mm above the highest electrode. Throughout extrusion, electrical impedance measurements were recorded at a rate of 1 frame/s^{-1}. An image pair from within the barrel is presented in Figure 10. The left-hand image is of the real part of the resistivity, and the right-hand image is of the

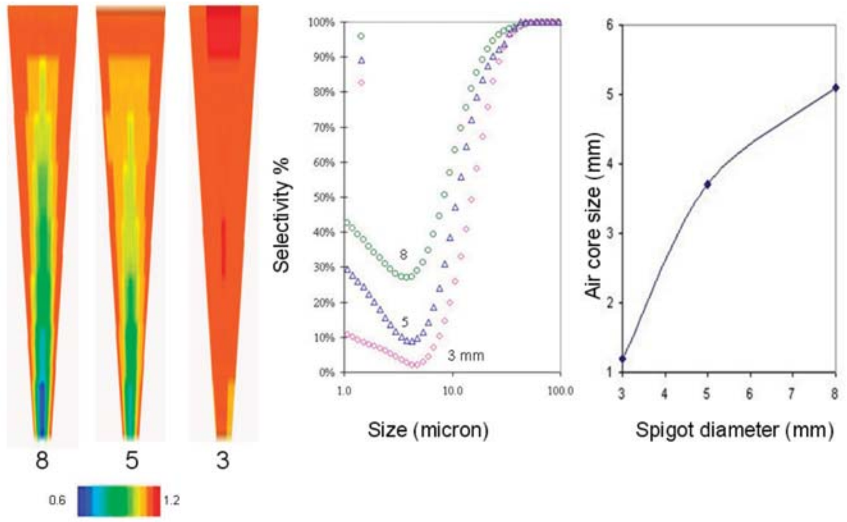

(a) (b) (c)

Figure 8—(a) Cross-sectional images through small (50 mm) diameter hydrocyclone and (b) measured selectivity function and (c) tomographically measured air core using the method described in[17], for 10 wt % slurry, mean size 18 microns for 8, 5 and 3 mm diameter spigots

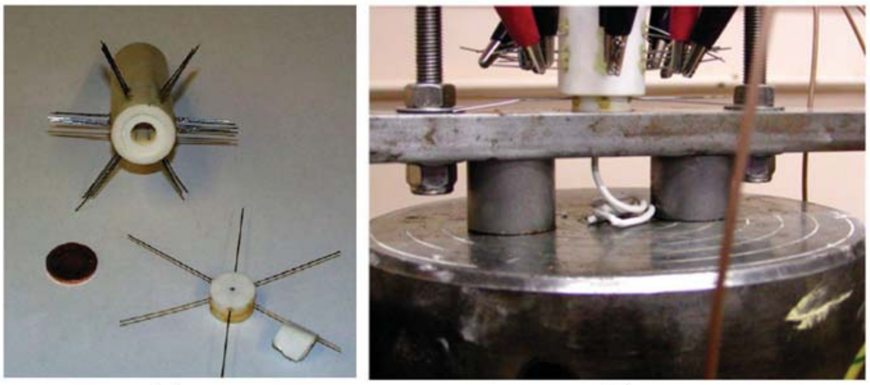

(a) (b)

Figure 9—(a) Electrode details within the extruder barrel and (b) extrusion process of α-alumina. (From [18])

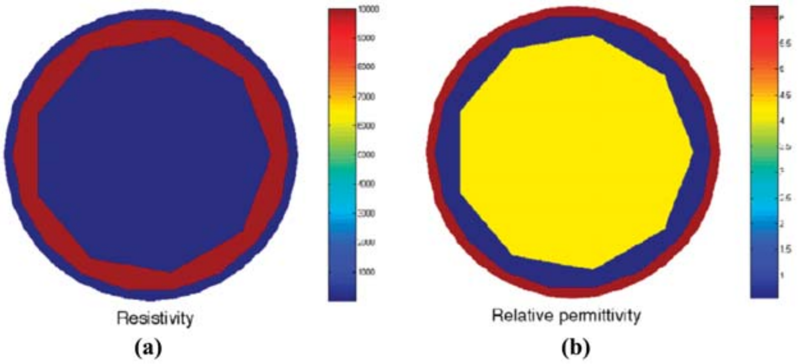

Figure 10—(a) Real and (b) imaginary parts of resistivity from extruder barrel (scale is relative when a two-dimensional approximation is used). (From [18])

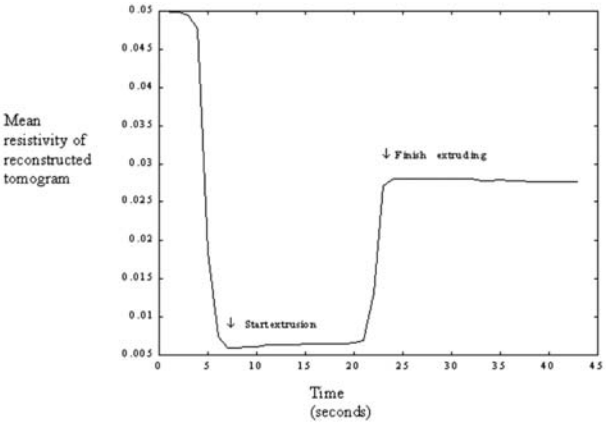

Figure 11—Trace of electrical resistance of paste from extruder barrel throughout an experiment. (From [18])

imaginary part, permittivity.

Once extrusion pressure is reached the reconstructed tomographic data reveal the key features: an outer ring of very low resistivity is apparent; an annulus of higher resistivity occurs just within this; and the central region again has lower resistivity. Impedance measurements can be used to monitor the development of a structure with the right moisture content (Figure11).

These data demonstrated how such methods can be applied to measurement homogeneity variations in a paste and from this infer structure. Use of additional information that could be estimated, such as local velocities, could offer significant new information for routine use. Sensing of the electrical 'texture' of multiphase mixtures has been applied at a larger length scale, e.g. in flotation columns and multiphase flows[19] and there is no physical reasons why such methods cannot be scaled down to examine some fluctuations in paste homogeneity as a routine measure.

Monitoring of mixing devices

Low speed impedance imaging

Stirred tank mixing was one of the earliest applications for EIT analysis relating to liquid-liquid, solid-liquid and multiphase systems (solid-liquid-gas). Early work demonstrated the quantification of impeller speed and type on mixing performance[1]. Here data collection times can be up to 50 frames of information per second, which is adequate for steady state and slowly changing systems but unsuited to observing kinetic effects in fast flowing systems.

In-pipe mixing is increasingly commonplace and of course has been used in solvent extraction (pulsed columns) for many years. In an analogous process, Figure 12 shows the application of online EIT to a so-called oscillatory baffled reactor (OBR). The main advantage of using the technology is that it facilitates performing certain reactions continuously within the process, which previously were possible only in many small batches[20].

OBRs are a new type of continuous reactor built of equally spaced orifice plate baffles. The main characteristic of these reactors is that the process fluid has an oscillatory movement that is superimposed on all the fluid in the reactor. This means that the direction of the fluid in the reactor is not following a linear movement. The addition of a sinusoidal imposed movement enables the radial mixing unlike the traditional plug flow reactors. A dual plane EIT sensor was used (Figure 12 (c)). Here an emulsions systems was explored (oil in water) and application of the reconstruction

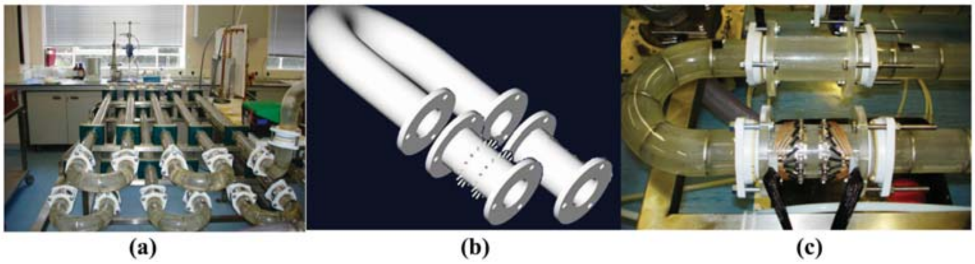
(a) (b) (c)

Figure 12—(a) OBR in the laboratory; (b) EIT sensor mechanical simulation and (c) its assembly in the OBR. (From [20])

algorithm enabled one to obtain the conductivity of the fluid in each one of the planes of electrodes. The values obtained from the tomographic measurement enable one to relate the characteristics of the emulsion such as concentration (C*v*) and with the parameters of control of the flow reactor[20].

The application of a cross-correlation method to the data obtained from the tomograms enabled (Figure 13) the velocity profiles in the X and Y planes of the dispersed phase in the OBR with the relation radius/diameter (r/D) of the pipe to be estimated.

Ultra-high speed imaging

Recent developments have enabled a much faster methods to be devised, suited to collecting temporally distinguishable information on flows up to 10 m/s. The demands of the applications range from a frame every few minutes to applications with fast evolving processes such as multiphase flows where frame rates of milliseconds or faster are desirable to observe the flow behaviour. The hardware of tomography systems has evolved to address the needs of certain applications that will benefit from these faster frame rates[21,22].

A dual plane EIT system that is capable of acquiring data at frame rates of around 1 000 dual-frames per second (dfps) has been developed[23] and applied to various flow problems. The methodology is transferring to the commercially available instrumentation (Industrial Tomography Systems plc) for examining fast reaction systems and integration of flow measurments to provide quantification of component mass flows.

The system has been used on the OBR[20] using nominal oscillatory frequencies between 0.5 Hz and 3 Hz. The reactor contained water and oil. The results of some tests are shown in Figure 15. The top left graph shows the average pixel conductivity at the two sensor planes. In this case the measurement shows that the planes have opposing changes in resistivity. This is due to an accumulation of oil at the top of the pipe, which is moved from one sensor plane to the next one. Only one plane is shown in the higher frequency graphs where the oscillatory resistivity changes reflect the faster oscillations of the reactor. The graphs clearly demonstrate the correlation of oil bubble concentration to the oscillatory frequency[23].

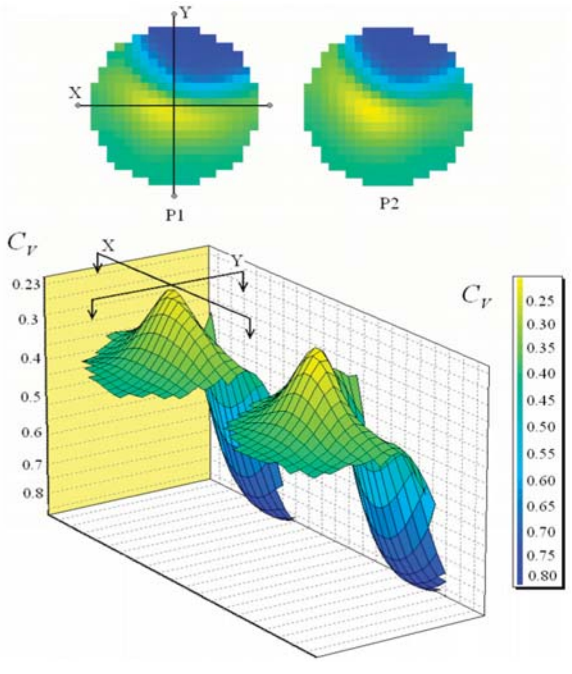

Figure 13—3D reconstruction of the oil volume distribution. (From [20])

Concluding remarks

The review has illustrated the manner is which impedance tomography can be used to abstract new information from slurry processes that can be used in modelling and online application. The information content can be used in a qualitative manner to detect transgressions from normal behaviour or in more detail to understand the process pathology. A particular opportunity lies in verification of chemical kinetic modelling, especially using the capabilities of the high speed systems illustrated above. This is relevant to mineral extraction, precipitation and reaction, phase changes and aging effects in transportation or storage.

There is a substantial and largely unmet need for velocity information and concentration information on opaque slurries. EIT is an emerging technique that can be used for mapping the concentration, and to measure velocity distributions in multiphase flows, where electrical conductivity or permeability differences exist. This is set to have real application in pipeline design and operation and, of course, in the fundamental design of a variety of minerals separation and related processes.

Acknowledgements

The authors acknowledge the support of Virtual Centre for Industrial Process Tomography and EPSRC Platform Grant EP/D031257/1.

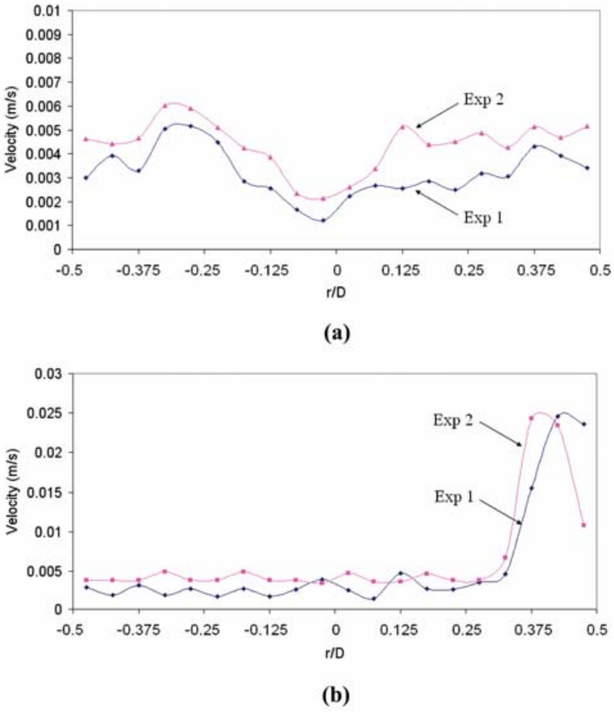

Figure 14—Local velocity distribution of the dispersed phase in (a) the plane X and (b) and plane Y. (From [20])

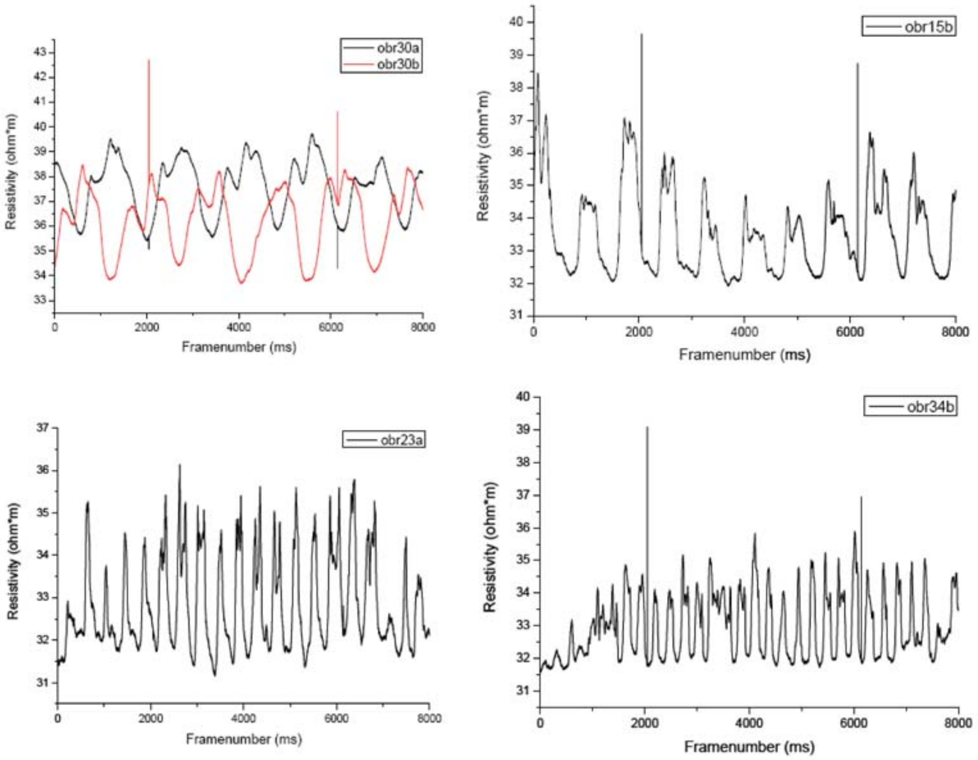

Figure 15—Average tomogram resistivities derived from high speed EIT system in an OSB reactor (pulsing at nominal frequencies of 0.5 Hz, 1 Hz, 2 Hz and 3 Hz). (From 23)

References

1. Williams, R.A. and Beck, M.S. *Process Tomography: principles, techniques, and applications*. Butterworth-Heinemann Ltd 1995.
2. Williams, R.A. *Mineral and material processing*, Process Imaging for Automatic Control, Scott DM, McCann H., Taylor and Francis, 2005. pp. 359–400.
3. Cullivan, J.C., Williams, R.A. and Cross, C.R. New insights into hydrocyclone operation, *Particulate Science and Technology*, vol. 21, 2003. pp. 83–103.
4. Fangary, Y.S., Abd El Ghani, A.S., El Haggar, S.M. and Williams, R.A. The effect of fine particles on slurry transport processes, *Minerals Engineering*, vol. 10, 1997. pp. 427–439.
5. Fangary, Y.S., Williams, R.A., Neil, W.A., Bond, J. and Faulks, I. Application of electrical resistance tomography to detect deposition in hydraulic conveying systems, *Powder Technology*, vol. 95, 1998. pp. 61–66.
6. Lucas, G.P., Cory, J., Waterfall, R.C., Loh, W.W. and Dickin, F.J. Measurement of the solids volume fraction and velocity distributions in solids–liquid flows using dual-plane electrical resistance tomography, *Flow Measurement and Instrumentation*, vol. 10, 1999. pp. 249–258.
7. Wang, M., Lucas, G., Dai, Y., Panayotopoulos, N. and Williams, R.A. Visualisation of bubbly velocity distribution in a swirling flow using electrical resistance tomography, *Particle & Particle Systems Characterization*, vol. 23, 2006. pp. 321–329.
8. Wang, M., Jones, T.F. and Williams, R.A. Visualization of asymmetric solids distribution in horizontal swirling flows using electrical resistance tomography, *Trans IChemE*, 81, Part A, 2003. pp. 854–861.
9. Halsey, D.M. Flow meters in swirling flows, *J Phys E: Sci Instrum*, vol. 20, 1987. pp. 1036–1040.
10. Jones, T.F. *Pipe design for improved particle distribution and reduced wear*, Directorate General Energy, ECSC 7220-EA/841, European Communities, Luxembourg. 1997.
11. Yin, W., Wang, M., Jones, T.F., Ganeshalingam, J., Williams, R.A., Miles, NJ., Li, D., Lai, Y. and Wu, Y. Measurement of swirling flow in hydraulic conveying using electrical resistance tomography, *Proceedings of the World Congress on Particle Technology IV*, Sydney, 21–25 July. 2002.
12. Nowakowski, A.F., Cullivan, J.C., Williams, R.A. and Dyakowski, T. Application of CFD to modelling of the flow in hydrocyclones. Is this a realizable option or still a research challenge?, *Minerals Engineering*, vol. 17, 2004. pp. 661–669.
13. Cullivan, J.C., Williams, R.A., Dyakowski, T. and Cross, C.R. New understanding of a hydrocyclone flow field and separation mechanism from computational fluid dynamics, *Minerals Engineering*, vol. 17, 2004. pp. 651–660.
14. Bennett, M.A. and Williams, R.A. Monitoring the operation of an oil/water separator using impedance tomography, *Minerals Engineering*, vol. 17, 2004. pp. 605–614.
15. Williams, R.A., Jia, X., West, R.M., Wang, M., Cullivan, J.C., Bond, J., Faulks, I., Dyakowski, D., Wang, S.J., Climpson, N., Kostuch, J.A. and Payton, D. Industrial monitoring of hydrocyclone operation using electrical resistance tomography, *Minerals Engineering*, vol. 12, 1999. pp.1245–1252.
16. Brennan, M., Holtham, P., Khanal, M. and Morrison, R. Comparing ERT Measurements with CFD Predictions for an Industrial Scale hydrocyclone classifier, *5th World Congress on Industrial Process Tomography,* Bergen, Norway. 2007.
17. West, R.M., Jia, X. and Williams, R.A. Parametric modelling in industrial process tomography, *Chem. Eng. J.*, vol. 77, 2000. pp. 31–36.
18. West, R.M., Scott, D.M., Sunshine, G., Kostuch, J., Heikkinen, L., Vauhkonen, M., Hoyle, BS., Schlaberg, H.I., Hou, R., and Williams, R.A. *In-situ* imaging of paste extrusion using electrical impedance tomography, *Meas. Sci. Technol.* vol. 13, 2002. pp. 1890–1897.
19. Bennett, M.A., West, R.M., Luke, S.P., Jia, X. and Williams, R.A. Measurement and analysis of flows in a gas-liquid column reactor, *Chemical Engineering Science*. vol. 54, 1999. pp. 5003–5012.
20. Vilar, G., Williams, R.A., Wang, M. and Tweedie, R.J. On Line Analysis of Structure of Dispersions in an Oscillatory Baffled Reactor using Electrical Impedance Tomography, *Chem. Eng. J.*, vol. 141, 2007. pp. 58–66.
21. Wang, M., Ma, Y., Holliday, N., Dai, Y., Williams, R.A. and Lucas, G. A High-Performance EIT System, *IEEE Sensors Journal*, vol. 5, 2005. pp. 289–299.
22. Wilkinson, A.J., Randall, E.W., Durrett, D.R., Naidoo, T. and Cilliers, J.J. The design of a 1000 frames/second ERT Data Capture System and Calibration Techniques Employed, *3rd World Congress on Industrial Process Tomography,* Banff, Canada. 2003.
23. Schlaberg, H.I., Jia, J., Qiu, C., Wang, M. and Li, H. Development and application of the Fast Impedance Camera—a high performance dual-plane electrical impedance tomography system, *Proceedings of the 5th International Symposium on Process Tomography*, Zakopane, Poland. 2008. ◆